Effect of density variation and non-covalent functionalization on the compressive behavior of carbon nanotube arrays

2011 Nanotechnology 22 425705

(http://iopscience.iop.org/0957-4484/22/42/425705)

Nanotechnology **22** (2011) 425705 (7pp) doi:10.1088/0957-4484/22/42/425705

Effect of density variation and non-covalent functionalization on the compressive behavior of carbon nanotube arrays

A Misra[1,2], J R Raney[2], A E Craig[2] and C Daraio[2]

[1] Instrumentation and Applied Physics, Indian Institute of Science, Bangalore, 560012, India
[2] Engineering and Applied Science, California Institute of Technology, Pasadena, CA 91125, USA

E-mail: daraio@caltech.edu

Received 22 July 2011, in final form 23 August 2011
Published 22 September 2011
Online at stacks.iop.org/Nano/22/425705

Abstract
Arrays of aligned carbon nanotubes (CNTs) have been proposed for different applications, including electrochemical energy storage and shock-absorbing materials. Understanding their mechanical response, in relation to their structural characteristics, is important for tailoring the synthesis method to the different operational conditions of the material. In this paper, we grow vertically aligned CNT arrays using a thermal chemical vapor deposition system, and we study the effects of precursor flow on the structural and mechanical properties of the CNT arrays. We show that the CNT growth process is inhomogeneous along the direction of the precursor flow, resulting in varying bulk density at different points on the growth substrate. We also study the effects of non-covalent functionalization of the CNTs after growth, using surfactant and nanoparticles, to vary the effective bulk density and structural arrangement of the arrays. We find that the stiffness and peak stress of the materials increase approximately linearly with increasing bulk density.

(Some figures in this article are in colour only in the electronic version)

1. Introduction

Carbon nanotube (CNT) arrays synthesized using a floating catalyst in a thermal chemical vapor deposition (TCVD) system have been reported to preserve their ability to recover and dissipate energy even after a large number of compressive cycles, similar to the behavior of foams [1–3]. The macroscopic mechanical response of freestanding CNT foams has been widely investigated [1–5]. These studies characterized both vertically aligned CNTs [1] and disordered CNT foams [4], focusing on their stress–strain response [1], fatigue [3], and time dependent behavior [5]. The earliest studies on the mechanical characteristics of bulk CNTs were predominantly limited to their quasi-static response [1], and their fatigue behavior in compression [3], without systematic correlation of the observed properties with structural characteristics of the materials (e.g. density, thickness or geometry). However, to transition the use of CNT foams from the laboratory scale to practical applications, it is important to be able to correlate their mechanical response to their structural characteristics, and to tailor their synthesis method to the specific operational conditions.

A few recent studies correlated the mechanical response of CNT-based structures with functional characteristics of the CNT arrays: for example, CNT sponges of variable density were created with controlled porosity [4], and CNT arrays have been assembled in multilayer stacks to enhance their impact energy absorption [6]. Recently, variations of the CNT arrays' bulk density, controlled during growth by the hydrogen concentration during synthesis, have been shown to affect the peak stress and energy absorption of the CNT arrays in compression [7]. The effect of density variation has also been shown to affect the bulk mechanical response of disordered (i.e. not aligned) CNT networks [4]. Here, we study the effect

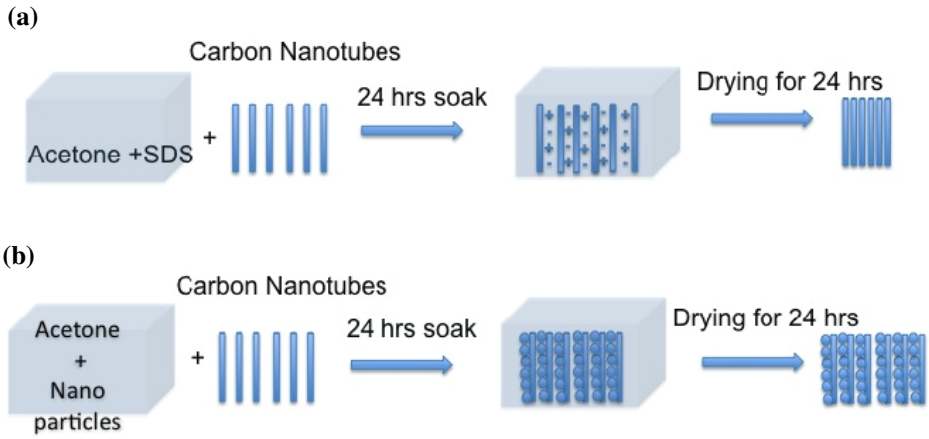

Figure 1. Schematic diagrams describing the wetting process of CNTs: (a) the freestanding carbon nanotubes are first soaked in the acetone/surfactant solution, and then dried. The CNTs densify by surface attraction. (b) Schematic diagram of the wetting of CNTs with a solution of acetone and nanoparticles.

of the carrier gas flow carrying the precursor on the structural and mechanical properties of vertically aligned CNT arrays, and we examine the effects of non-covalent functionalization of the CNT surfaces on the bulk mechanical response of the arrays in compression. The addition of surfactant (SDS) and the attachment of silica (SiO_2) nanoparticles to the CNT walls are employed to control the microstructural arrangement of the CNTs in the arrays, and to tune the mechanical response of the arrays after growth.

2. Experimental section

Vertically aligned arrays of carbon nanotubes were grown using a floating catalyst TCVD method [2]. The microstructure of the resulting arrays was highly hierarchical: at the meso-scale, CNT bundles grew vertically away from the substrates; at the micro-scale (within these bundles), the individual CNTs grew highly entangled with their neighbors. The TCVD system used consisted of a single furnace utilizing a quartz tube through which the precursor vapors passed into the heating zone. Source precursors (0.02 g ferrocene per milliliter of toluene) were fed directly into the quartz tube before entering the heating zone. The growth substrates consisted of silicon wafers with a 1 μm thick thermal oxide layer (area $\sim 3 \times 2$ cm^2), and were placed at the center of a high temperature (825 °C) zone in the furnace. After the growth was completed, small sections of the CNT arrays ($\sim 7 \times 7$ mm^2) were separated from the substrates using a razor blade, to obtain freestanding samples for the testing. The bulk densities of the freestanding samples were calculated by dividing the measured mass of each sample by its measured volume. The density of the CNT samples was found to vary between 0.12 and 0.28 g cm^{-3}, depending on the position of the CNT sections on the growth substrate with respect to the carrier gas flow direction (CNT arrays grown in the substrate's sections closer to the gas inlet had higher densities).

The CNT arrays were functionalized by two methods: in the first one, the CNT arrays were first separated from the growth substrate and then they were wetted in 15 ml of volatile acetone containing 0.02 g of dispersed silica nanoparticles (with diameters ∼10–20 nm); in the second one, the CNT arrays were also first separated from the growth substrate and then they were immersed in acetone containing sodium dodecyl sulfate (SDS) instead of the silica (SiO_2) particles. The solutions containing acetone and nanoparticles or surfactant were ultrasonicated for 30 min to obtain uniform dispersions. The freestanding CNT samples were soaked in the ultrasonicated solutions for 24 h and they were dried for the next 24 h. The schematic diagrams in figures 1(a) and (b) describe the wetting process of CNTs in acetone with dispersed SDS and SiO_2 nanoparticles, respectively. The mechanisms of the observed structural changes in the CNT arrays after functionalization are described in section 3.

3. Results and discussion

Before mechanical testing, the as-grown and chemically treated CNT samples were analyzed with high resolution scanning electron microscopy (HR-SEM), to identify emerging microstructural features caused by the different preparation processes. A typical SEM image acquired from the as-grown CNTs is shown in figure 2(a). We first studied the effect of acetone wetting on the microstructure of the CNT arrays, without the addition of surfactant or nanoparticles. The samples showed the formation of typical crack patterns (figure 2(b)), resulting after evaporation of the liquid. The formation of such patterns on wetted CNT arrays was reported earlier, and was attributed to the presence of strong capillary forces during the liquid evaporation [8, 9]. The schematic diagram in the inset of figure 2(b) describes the representative structural rearrangement of the CNTs after acetone evaporation. Wetting (and subsequently drying) the CNT samples with a mixture of surfactant (SDS) and acetone was found to result in a significantly different microstructure (figure 2(c)). In this case, the CNTs in the array appeared to form dense bundles, emerging from the combination of van der Waals interactions and ionic charges on the CNTs' surfaces induced by the random attachment of

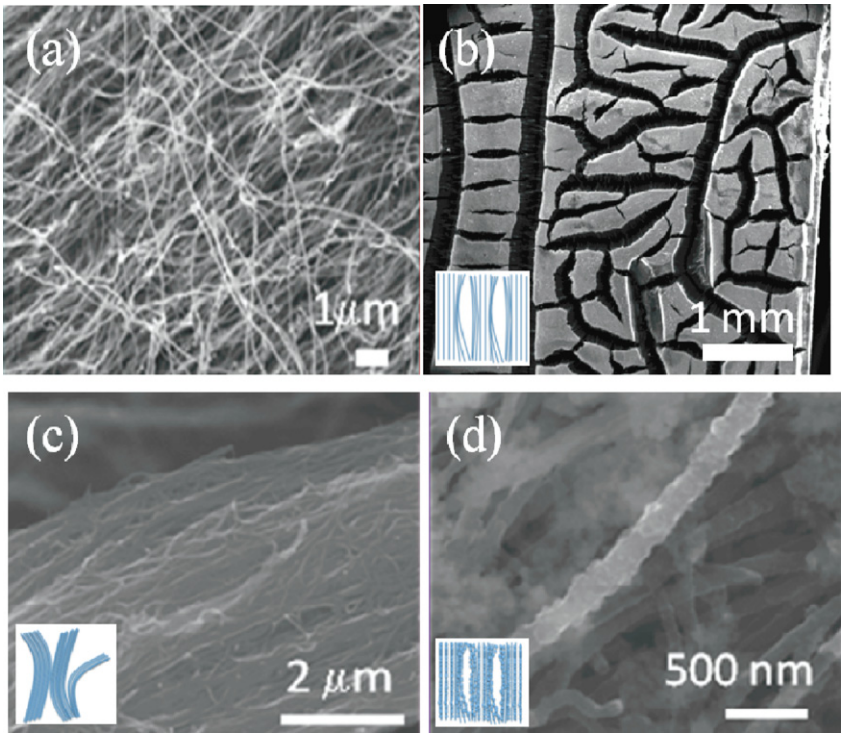

Figure 2. Scanning electron microscope images of untreated and chemically treated carbon nanotube arrays: (a) microstructure of the as-grown carbon nanotube arrays prior to being functionalized. (b) Top-view of the surface of a CNT array showing macroscopic cracks formed in the freestanding samples after being wetted with acetone and dried in air. (c) Microstructure of a CNT sample treated with acetone and SDS surfactant; carbon nanotubes form dense bundles. (d) Microstructure of a CNT sample wetted with silica nanoparticles; after the drying process, nanoparticles adhere to the surface of individual carbon nanotubes. The schematic representations in the insets describe the structural modifications occurring in the CNT samples.

surfactant molecules [10], as shown in the schematic diagram figure 1(a). The schematic diagram in the inset of figure 2(c) shows the idealized densification and partial bending of the CNTs. The microstructural effects resulting from wetting (and subsequent drying) of the CNT arrays with a mixture of acetone and SiO_2 nanoparticles can be seen in figure 2(d). It is evident that the SiO_2 nanoparticles (of diameter ∼10–20 nm) attach uniformly to the CNTs' surfaces, without the need for additional functionalization or chemical treatment. The schematic diagram in the inset of figure 2(d) represents the attachment of nanoparticles on the CNT surfaces and their idealized microstructural rearrangement, with no densification and bending observed.

The density gradient measured in the as-grown CNT arrays as a function of the position on the growth substrate is shown in figure 3(a). The black arrow indicates the direction of the gas flow inside the chamber with respect to the substrate position. From the diagram it is evident that the as-grown CNTs' density is higher in the substrate regions closer to the gas flow input, and it decreases gradually as the CNTs grow farther from the flow input.

We measured the mechanical response of the samples as a function of density variation and chemical functionalization. Quasi-static compression tests were performed on the samples at four different strain rates, 50%, 3%, 0.3%, and 0.03% s^{-1} to a maximum strain of 50%. We first tested the mechanical response of the as-grown CNT samples obtained from the same growth substrate, to study the effects of density variations during growth, as a function of their position on the substrate. We calculated the elastic modulus of the samples by fitting the initial linear portion of the stress–strain curve at low strain. The measured compressive moduli and the peak stresses are shown in figures 3(b) and (c) as a function of density. The tables shown in the insets refer to the samples' position on the growth substrate, and the different marker shapes indicate the different strain rates of testing for each sample. We noted that the compressive modulus and the peak stress vary linearly with density, while the strain rate has a negligible effect, as evident in figures 3(d) and (e). We confirmed the linear dependence of the CNT arrays' mechanical response on density, and the absence of strain rate effects, by testing a large number of CNT samples obtained from different growth substrates in separate synthesis processes, with densities ranging from 0.12 to 0.28 g cm^{-3}. Figure 3(f) shows the linear dependence of the compressive modulus on bulk density where the data for each strain rate were fitted to the following equation

$$E = k_1 d + k_2. \tag{1}$$

Here, E is the measured elastic modulus, d is the CNT bulk density, and $k_{1,2}$ are the fitting parameters. Similarly, figure 3(g) shows the linear dependence of peak stress on density where the data for each strain rate were fitted to the

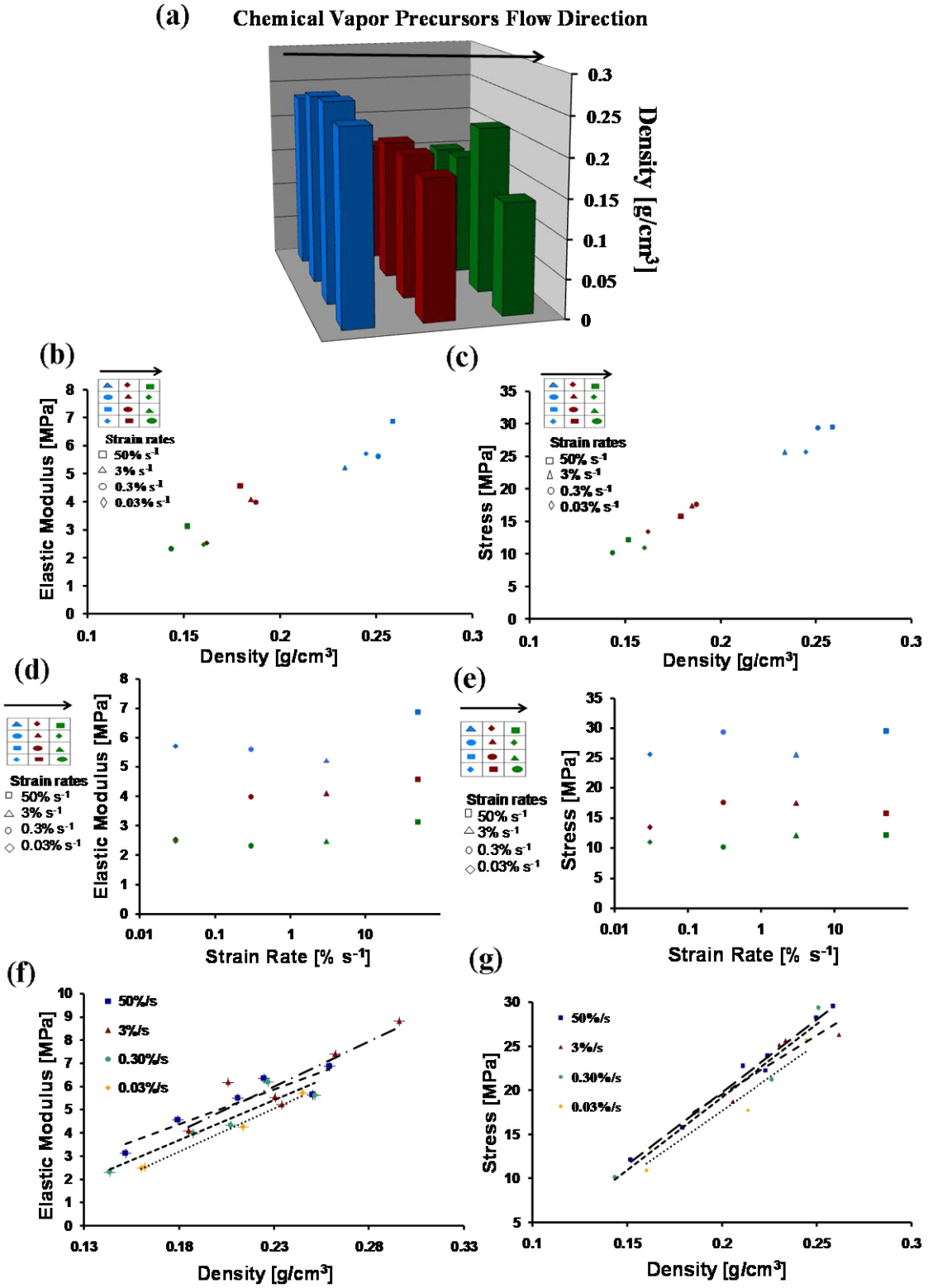

Figure 3. Mechanical response of as-grown carbon nanotubes: (a) density variation of the as-grown carbon nanotubes as a function of the position on the substrate. The black arrow on top indicates the direction of the chemical precursors' flow. (b) Elastic modulus at small strains as a function of the density for the freestanding carbon nanotubes. Four different strain rates, 50% s^{-1} (square marker), 3% s^{-1} (triangular marker), 0.3% s^{-1} (circular marker), and 0.03% s^{-1} (diamond marker) were used on each portion of the sample grown concurrently; the inset diagrams report the relative position of each tested sample on the growth substrate. (c) Measured peak stress as a function of density of the carbon nanotubes at four strain rates (50–0.03% s^{-1}) (d). (e) Elastic modulus and peak stress values as a function of strain rate, respectively. (f), (g) Mechanical response of freestanding carbon nanotubes in a larger number of randomly selected samples: (f) elastic modulus and (g) peak stress plotted for four different strain rates, 50% s^{-1} (blue squares), 3% s^{-1} (red triangles), 0.3% s^{-1} (green circles), and 0.03% s^{-1} (yellow diamonds) as a function of samples' density. The data points for each strain rate were fitted with a linear function.

Table 1. The table reports the values for the fitting parameters used in equations (1) and (2) describing the linear-fit trend shown in figures 3(f) and (g).

Strain rate (% s^{-1})	k_1	k_2	k_3	k_4
0.03	37.414	−3.5535	150.74	−12.442
0.3	34.589	−2.5387	165.69	−13.894
3	38.556	−2.8682	133.62	−7.1712
50	30.013	−1.0339	164.51	−13.097

following equation

$$\sigma = k_3 d + k_4. \quad (2)$$

Here, σ is the peak stress, d is the density, and $k_{3,4}$ are the fitting parameters. The fitting parameters $k_{1,2,3,4}$ are summarized in table 1.

After testing the as-grown samples, we characterized the properties of the chemically treated samples. We found that the surface functionalization, with non-covalent attachment of surfactants and SiO_2 nanoparticles, can alter the bulk density, influencing the mass and/or the volume of the samples. Table 2 summarizes specific changes in mass, height, and surface area after wetting and drying the CNT samples with acetone, acetone/surfactants, and acetone/silica nanoparticles. We measured two sets of samples (S1 and S2) for each type of functionalization. Changes in the overall mass of the samples were observed after wetting with surfactant and silica nanoparticles, while no mass changes occurred after treatment with only acetone. The CNT samples' height and surface area were reduced when the samples were treated with acetone and acetone/surfactants. This is likely due to the densification, and hence partial bending, of the CNTs (see figures 2(b) and (c), respectively). CNT samples treated with solutions of acetone and silica nanoparticles did not present any evident dimensional change. The densification in this case can be assumed to be negligible due to the repulsive effects originating from the presence of negative zeta potential [11] between the SiO_2 particles on the surface of the CNTs.

We analyzed the mechanical response of the surface modified CNT samples using the same experimental conditions described above. Results obtained with quasi-static compression tests performed on CNT samples treated with acetone and surfactant (SDS), compared with as-grown, freestanding CNTs are shown in figure 4. In the graph, the vertical axis shows the measured peak stress, and the horizontal axis shows the different strain rates used for testing. The samples (four sets of wetted and as-grown CNT control) arrays are compared side-by-side at each strain rate (all experimental tests at the same strain rate are encircled by dotted lines). The measured peak stresses are clearly higher for the functionalized CNTs than they are for the non-functionalized CNTs at all strain rates tested. The average peak stress was measured from the six measurements performed on six randomly selected samples, with the error bars in figure 4 representing the corresponding standard deviation. These deviations are a result of density variations in the selected samples. The results show no specific trend with strain rate. The higher peak stress level observed in samples functionalized

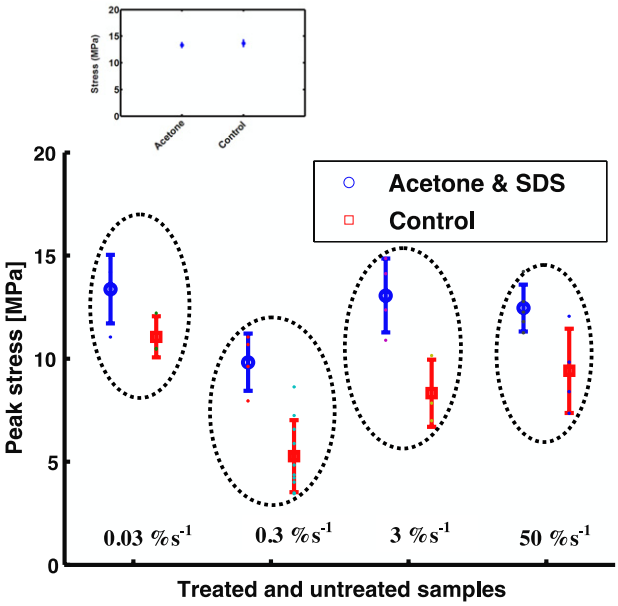

Figure 4. Comparison of the maximum value of compressive peak stress in samples wetted with surfactant (data points denoted by circles) and in freestanding, as-grown CNTs (control) (data points denoted by squares), at varying strain rates. The inset shows a comparison between CNT samples wetted with only acetone and as-grown CNTs. Each circle represents tests from a different strain rate (indicated on the x-axis).

Table 2. The table reports the values of bulk density measured before (initial) and after (final) wetting CNTs with acetone, surfactant/acetone, and SiO_2/acetone. For each value we synthesized and measured two samples of CNTs (S1 and S2). A list of mass, height, and area is shown for the pristine and treated CNTs.

Measured quantities		CNTs/acetone	CNTs/acetone/surfactant	CNTs/acetone/silica particles
Mass (g) $\times 10^{-2}$ (initial/final)	S1	1.75/1.73	1.64/1.77	1.52/1.62
	S2	1.89/1.9	2.07/2.17	1.9/2.0
Height (mm) (initial/final)	S1	1.94/1.87	1.79/1.76	1.78/1.77
	S2	1.86/1.82	1.90/1.85	1.87/1.87
Area (mm^2) (initial/final)	S1	37.21/36.56	44.54/43.12	41.83/41.78
	S2	43.62/43.49	41.01/40.57	42.9/43.20
Density (g cm^{-3}) (initial/final)	S1	0.25/0.25	0.21/0.23	0.20/0.22
	S2	0.23/0.24	0.27/0.29	0.24/0.25

with surfactant could be related to the densification of the structure as a result of the surface modification. Details of the interaction of surfactant (specifically SDS) with CNTs can be found in earlier studies [12–14]. SDS has widely been used to disperse individual hydrophobic carbon nanotubes by providing anionic surface charge in the liquid medium [15]. SDS was also reported to densify the CNTs on the growth substrate, through capillary forces emerging when the liquid penetrates into the pores of the CNT structure [16]. In our case, we process freestanding CNT samples (not attached to a growth substrate). This allows the nanotubes to densify after the acetone evaporates. The same treatment applied on as-grown samples not separated from the substrate could result in different microstructures and reduced densification [8, 9]. The mechanism of surface functionalization of single wall CNTs with SDS was studied numerically [14]. It was found that SDS molecules form a random network on the CNT surfaces [14]. This disorder could cause a non-uniform distribution of charges on the CNT surfaces, and the CNT densification is expected to result from the attraction of oppositely charged clusters. After acetone evaporates the layers of surfactant remain attached around the CNT surfaces. It was reported that the concentration of SDS attached on the CNTs surfaces increases with increasing CNT diameter [14]. The study by Namilae *et al* reported that the stress experienced by the CNTs increases significantly with the number of adhering molecules to the surface, because the applied load can be transferred more effectively between adjacent nanotubes through the attached molecule, which in our case is surfactant [17]. The higher values of peak stress observed in our experiments for the functionalized CNT arrays can be explained by a similar interaction mechanism of stress transfer between CNTs. The presence of SDS molecules wrapped around the CNTs' outer walls enhances ionic interactions between adjacent CNTs and distributes the applied load more effectively than the van der Waals interfacial interaction present in the as-grown, freestanding CNTs. The advantage of non-covalent functionalization compared to covalent functionalization, results from the presence of fewer defect sites on the CNTs walls, which would weaken the overall CNT structure.

The functionalization with SDS neither affects the elastic bending response of the CNT arrays nor the buckling stress, as these deformations rely less on interfacial interactions between CNTs. The details of the compressive response of CNTs including buckling and post-buckling regimes can be found elsewhere [6]. For comparison, we also studied the compressive response of CNT arrays wetted with acetone only (no surfactants included). As shown in figure 2(b), the acetone wetting, and the subsequent drying, causes the formation of characteristic cracks on the surface of the CNTs. The mechanical response of these samples is shown in the inset of figure 4, together with the data acquired from the as-grown freestanding CNT arrays (control). We have not observed any difference in the peak stress values reached in the compression of the acetone wetted and the control samples after 50% strain, at the same rate (50% s^{-1}). This shows that the increase in peak stress observed for the CNTs treated with SDS is primarily due to the non-covalent functionalization.

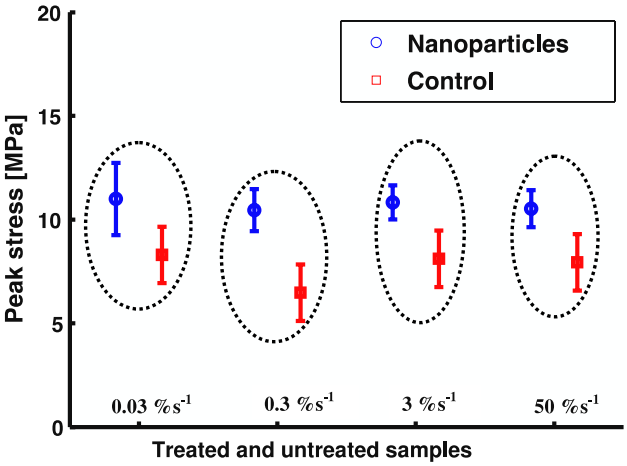

Figure 5. Variation of measured peak stress as a function of strain rate. Data points shown by circles represent samples with nanoparticles, and squares represent the results obtained from the as-grown (control) samples. Each circle represents tests from a different strain rate (indicated on the x-axis).

Finally, we tested the mechanical response of CNTs wetted with the solution of acetone and SiO_2 nanoparticles, and dried. The dispersion property of silica nanoparticles in organic media has been studied in detail [11]. It was shown that uniform dispersion in the solution is a result of the higher zeta negative potential, leading to repulsive effects between the particles [11]. The resulting uniform particle distribution on the CNTs' surfaces (figure 2(d)) is driven by acetone modified surface interactions [18] between the silica particles and the carbon nanotubes. Rance *et al* [19] showed that the particle affinity to attach to nanotubes increases with the diameter and length. This could explain the high affinity found in our ∼2 mm long CNTs. The quasi-static mechanical response of CNTs coated with SiO_2 nanoparticles is shown in figure 5. These samples were extracted from the same growth substrate and randomly selected for the nanoparticles attachment. The measured peak stresses are compared (similarly as in figure 4) among pristine CNT samples and those coated with nanoparticles. The level of peak stress reached in CNT samples coated by SiO_2 nanoparticles is higher as compared to untreated, freestanding CNTs. This behavior is in agreement with the results shown in figure 4 for a large number of randomly selected samples modified with surfactant. In particular, the stiffening provided by the particles on the surface of the CNTs plays a crucial role in the densification regime. The magnitude of the stress enhancement obtained with the CNT functionalization with SiO_2 nanoparticles is nearly the same as that of the SDS functionalized CNTs. The effect of the strain rate was found to be negligible in the range tested in our experiments (0.03%–50% s^{-1}).

4. Conclusions

In conclusion, we have studied the effect of density variation and surface functionalization on the compressive mechanical

responses of carbon nanotube arrays. We have identified a density gradient in the thermal CVD synthesis of CNTs, determined by the sample position on the substrate in the reactor, relative to the carrier gas flow direction. We tested the samples under quasi-static compression at different loading rates. The peak stress and the modulus of the as-grown, freestanding CNT arrays were found to increase linearly with density. We have controlled the CNT array density and microstructural organization with non-covalent functionalization and silica nanoparticle surface modification. In both cases the stiffness has been found to increase from the as-grown (control) samples. This study opens new avenues for controlling the mechanical response and microstructural properties of freestanding CNT arrays.

Acknowledgments

This work is supported by the Institute for Collaborative Biotechnologies, under contract W911NF-09-D-0001 with the Army Research Office. J R R also gratefully acknowledges support from the Department of Defense via a National Defense Science and Engineering Graduate (NDSEG) fellowship.

References

[1] Cao A, Dickrell P L, Sawyer W G, Ghasemi-Nejhad M N and Ajayan P M 2005 Super-compressible foam like carbon nanotube films *Science* **310** 1307–10

[2] Misra A, Greer J R and Daraio C 2009 Strain rate effects in the mechanical response of polymer-anchored carbon nanotube foams *Adv. Mater.* **21** 334–8

[3] Suhr J, Victor P, Ci L, Sreekala S, Zhang X, Nalamasu O and Ajayan P M 2007 Fatigue resistance of aligned carbon nanotube arrays under cyclic compression *Nature Nanotechnol.* **2** 417–21

[4] Gui X, Cao A, Wei J, Li H, Jia Y, Li Z, Fan L and Wang K 2010 Soft, highly conductive nanotube sponges and composites with controlled compressibility *ACS Nano* **4** 2320–6

[5] Deck C P, Flowers J, McKee G S B and Vecchio K 2007 Mechanical behavior of ultralong multiwalled carbon nanotube mats *J. Appl. Phys.* **101** 023512

[6] Misra A, Raney J R, De Nardo L, Craig A and Daraio C, Synthesis and characterization of carbon nanotube-polymer multilayer structures in review

[7] Raney J R, Misra A and Daraio C 2011 Tailoring the microstructure and mechanical properties of arrays of aligned multiwall carbon nanotubes by utilizing different hydrogen concentrations during synthesis *Carbon* **49** 3631–8

[8] Chakrapani N, Wei B, Carrillo A, Ajayan P M and Kane R S 2004 Capillarity-driven assembly of two-dimensional cellular carbon nanotube foams *Proc. Natl Acad. Sci.* **101** 4009–12

[9] Kaur S, Sahoo S, Ajayan P M and Kane R 2007 Capillarity-driven assembly of carbon nanotubes on substrates into dense vertically aligned arrays *Adv. Mater.* **19** 2984–7

[10] Yurekli K, Mitchell C A and Krishnamoorti R 2004 Small-angle neutron scattering from surfactant-assisted aqueous dispersions of carbon nanotubes *J. Am. Chem. Soc.* **126** 9902–3

[11] Du M and Zheng Y 2007 Modification of silica nanoparticles and their application in UDMA dental polymeric composites *Polym. Compos.* **28** 198–207

[12] O'Connell M J *et al* 2002 Band gap fluorescence from individual single-walled carbon nanotubes *Science* **297** 593–6

[13] Arnold M S, Green A A, Hulvat J F, Stupp S I and Hersam M C 2006 Sorting carbon nanotubes by electronic structure using density differentiation *Nature Nanotechnol.* **1** 60–5

[14] Tummala N R and Striolo A 2009 SDS surfactants on carbon nanotubes: aggregate morphology *ACS Nano* **3** 595–602

[15] Vaisman L, Wagner H D and Marom G 2006 The role of surfactants in dispersion of carbon nanotubes *Adv. Colloid Interface Sci.* **128** 37–46

[16] Zhou J J, Noca F and Gharib M 2006 Flow conveying and diagnosis with carbon nanotube arrays *Nanotechnology* **17** 4845–53

[17] Namilae S and Chandra N 2006 Role of atomic scale interfaces in the compressive behavior of carbon nanotubes in composites *Compos. Sci. Technol.* **66** 2030–8

[18] Ellisa V, Vijayamohanan K, Goswami R, Chakrapani N, Ramanathan L S, Ajayan P M and Ramanath G 2003 Hydrophobic anchoring of monolayer-protected gold nanoclusters to carbon nanotubes *Nano Lett.* **3** 279–82

[19] Rance G A, Marsh D H, Bourne S J, Reade T J and Khlobystov A N 2010 van der Waals interactions between nanotubes and nanoparticles for controlled assembly of composite nanostructures *ACS Nano* **24** 4920–8